Taylor & Francis
Taylor & Francis Group

ADDENDUM

Check for updates

An interconnection between tip-focused Ca^{2+} and anion homeostasis controls pollen tube growth

Sarah Herbell, Timo Gutermuth, and Kai Robert Konrad

University of Wuerzburg, Julius-Von-Sachs Institute for Biosciences, Department of Botany I, Wuerzburg, Germany

ABSTRACT

Plant reproduction is the basis for economically relevant food production. It relies on pollen tube (PTs) growth into the female flower organs for successful fertilization. The high cytosolic Ca^{2+} concentration ([Ca^{2+}]$_{cyt}$) at the PT tip is sensed by Ca^{2+}-dependent protein kinases (CPKs) that in turn activate R- and S-type anion channels to control polar growth. Lanthanum, a blocker for plant Ca^{2+}-permeable channels was used here to demonstrate a strict dependency for anion channel activation through high PT tip [Ca^{2+}]$_{cyt}$. We visualized this relationship by live-cell anion imaging and concurrent triggering of Ca^{2+}-elevations with the two-electrode voltage-clamp (TEVC) technique. The anion efflux provoked by a TEVC-triggered [Ca^{2+}]$_{cyt}$ increase was abolished by Lanthanum and was followed by an overall rise in the cytosolic anion concentration. An interrelation between Ca^{2+} and anion homeostasis occurred also on the transcript level of CPKs and anion channels. qRT-PCR analysis demonstrated a co-regulation of anion channels and CPKs in media with different Cl$^-$ and NO$_3^-$ compositions. Our data provides strong evidence for the importance of a Ca^{2+}-dependent anion channel regulation and point to a synchronized adjustment of CPK and anion channel transcript levels to fine-tune anion efflux at the PT tip.

Introduction

It is well established that PT growth depends on a cytosolic Ca^{2+}-gradient with high [Ca^{2+}]$_{cyt}$ at the very tip. How this [Ca^{2+}]$_{cyt}$ gradient orchestrates PT growth and guidance to accomplish successful fertilization is largely unknown.[1,2] Cyclic nucleotide gated channel 18 (CNGC18) and glutamate receptor-like channels are considered to be prime candidate Ca^{2+}-entry channels mediating Ca^{2+}-influx at the tip of PTs.[3,4] CNGC18 harbors typical electrophysiological features of so-called hyperpolarization activated Ca^{2+}-channels (HACCs), which were identified in PT- and pollen grain protoplasts with the patch-clamp technique.[5–7] We recently applied short hyperpolarizing voltage pulses (−200 mV), known to activate HACCs, with the two electrode voltage-clamp (TEVC) technique to demonstrate that Ca^{2+}-permeable channel activity is confined to the PT tip.[8] A double barreled glass microelectrode is thereby inserted into a growing PT to perform voltage-clamping, which enables us to set the membrane voltage to defined values while performing Ca^{2+}-imaging. Moreover, we could establish that Ca^{2+}- and anion homeostasis are tightly linked to promote PT growth since an artificial Ca^{2+}-increase triggered by the TEVC technique or induced pharmacologically was followed by high anion channel activity and a decrease in tip anion concentration.[8,9] Previous studies characterized anion efflux from the grain and the PT tip to be essential for germination and polar growth.[10,11] In Gutermuth et al., 2018, we identified three Ca^{2+}-dependent protein kinases (CPKs), namely CPK2/20/6 to relay the high tip [Ca^{2+}]$_{cyt}$ information for activating R-(rapid) and S-(slow) type anion channels at the PT tip, namely slow anion channel1 homolog 3 (SLAH3), aluminum-activated malate transporter 12 (ALMT12), ALMT13 and ALMT14. Multiple anion channel and CPK loss-of-function mutants are compromised in anion currents as well as *in vitro* and *in vivo* PT growth.[8] This pointed out that the Ca^{2+}-signaling pathway for anion channel activation via CPK2/20/6 plays an important role in successful fertilization and both, channels and kinases, to represent positive regulators of PT growth.[8] The exact role of anion fluxes in PT growth is still speculative, as well as their integration in the signaling network to promote growth. In this manuscript, we substantiated the essential role of [Ca^{2+}]$_{cyt}$ in anion channel activation at the PT tip by pharmacological means and show that an interrelation between anion and Ca^{2+}-homeostasis exists on the transcript level, too. The anion channel and CPK expression patterns in media with different anion contents are consistent with a regulation of R- and S-type channels by CPKs as well as intra- and extracellular Cl$^-$ or NO$_3^-$ to maintain sufficient tip anion efflux.

Results

We have recently established a novel approach to trigger apical [Ca^{2+}]$_{cyt}$ elevations in PTs via 1 sec lasting −200 mV pulses applied with the TEVC technique.[8] Application of such

voltage pulses and simultaneous live-cell imaging was used here to monitor Ca^{2+}-induced anion release at the PT tip to study the dynamic interdependence of $[Ca^{2+}]_{cyt}$ and $[anion]_{cyt}$ in more detail. If anion channel activation solely relies on high $[Ca^{2+}]_{cyt}$ at the PT tip the presence of Lanthanum, an inhibitor of plant Ca^{2+}-permeable channels,[12,13] should prevent anion efflux. To test this hypothesis, Cl^--Sensor[14] expressing tobacco PTs were impaled with double-barreled glass microelectrodes (Figure 1, left side). Under voltage-clamp conditions we were able to trigger $[Ca^{2+}]_{cyt}$ increases while monitoring $[anion]_{cyt}$ dynamics. To display the $[anion]_{cyt}$ dynamics over time, a false-color coded kymograph was generated from the fluorescence resonance energy transfer (FRET)-based sensor signal along the PT (Figure 1, right side). As expected, five repetitive −200 mV voltage pulses with an interval time of 15 sec triggered an apical reduction in ratio signal implying $[anion]_{cyt}$ decrease via a Ca^{2+}-dependent mechanism. Five depolarizing voltage pulses (+ 60 mV) with the same duration and interval time failed to induce a decrease in tip $[anion]_{cyt}$ (Figure 1). This is in agreement with electrophysiological characteristics of HACCs which are unable to mediate Ca^{2+}-influx at positive membrane potentials. The application of 100 μM $LaCl_3$ during a second series of repetitive hyperpolarization voltage pulses abolished the rhythmic tip $[anion]_{cyt}$ release progressively within 3–4 min and induced an overall $[anion]_{cyt}$ accumulation within the apex after 5 min of inhibitor treatment (Figure 1, right panel, n = 9). The second phase of repetitive −200 mV pulses had longer interval times (20 sec voltage-pulse interval instead of 15 sec) to avoid excessive anion release over time attenuating the overall Cl^--Sensor signal.

Since a rise in anion concentration of the PT growth medium causes the overall $[anion]_{cyt}$ and additionally the Ca^{2+} gradient to increase,[9] we speculated whether $[anion]_{cyt}$ feedback on components of the Ca^{2+}-signaling pathway. If an interconnection between $[Ca^{2+}]_{cyt}$ and $[anion]_{cyt}$ homeostasis exists, they should be regulated in concert either biochemically, transcriptionally or both. Hence, we quantified transcript levels of in vitro grown PTs of all R- and S-type anion channel genes, as well as CPKs known to be associated with anion homeostasis.[8] Because R- and S-type anion channels have been reported to harbor distinct conductivities for different anions,[15–17] we used three different PT growth media with discrete anion compositions to study the interrelation between CPK and anion channel transcripts. Media with high (40 mM) Cl^- and NO_3^- content were used since they result in high PT R- and S-type anion currents, respectively.[8] Clade III members of the ALMT family comprise ALMT11/12/13/14, with the latter three proteins representing plasma membrane anion channel (sub) units.[8] In the absence of the organic anion malate, a transcriptional enhancer of ALMT clade III genes,[8] ALMT12 is well expressed and showed strongest expression in high NO_3^- medium (Figure 2A). In contrast, the expression profile of ALMT13 appeared very different. ALMT13 transcript levels were close to the detection limit in high NO_3^- medium, however, it was 60 (p < 0.0269) and 40-fold (p < 0.0178) upregulated in high Cl^- and Cl^-/NO_3^- minimal medium, respectively (Figure 2A). The expression profiles of ALMT14 was not significantly altered among the three different media and was close to the detection limit. ALMT3 and ALMT4 which are medium and low expressed, respectively, belong to the tonoplast localized clade II and are thus not considered here to play a major role in plasma membrane anion transport at the apex. Interestingly, they both show the tendency to be lower expressed in high Cl^- medium compared to high NO_3^- and Cl^-/NO_3^- minimal medium (Figure 2A). Among the members of the SLAC/SLAH anion channel family, only SLAH3 is expressed (Figure 2B). SLAH3 transcript numbers were significantly upregulated in high Cl^- medium in comparison to the
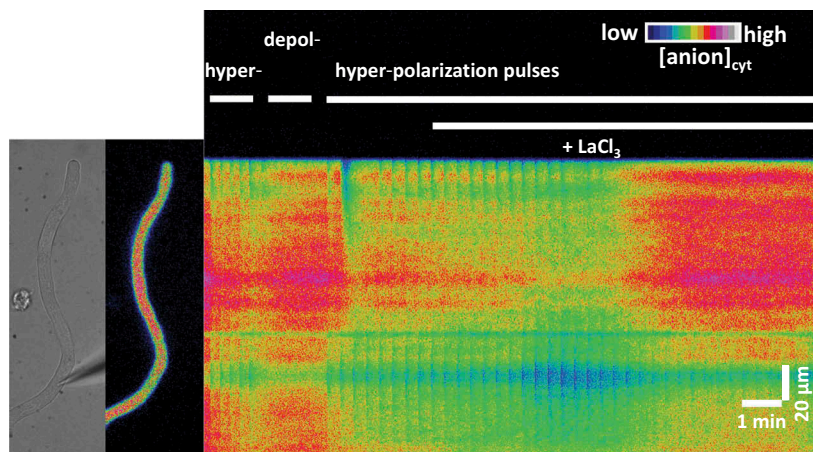

Figure 1. Pollen tube tip anion release depends on apical Ca^{2+}-channel activity. The TEVC technique was used simultaneously with live-cell anion imaging with a FRET-based Cl^--Sensor during repetitive −200 mV induced $[Ca^{2+}]_{cyt}$ increases in PTs. A brightfield and false color-coded FRET-ratio image of a PT expressing the Cl^--Sensor is shown (left). One kymograph of a representative cytosolic anion concentration ($[anion]_{cyt}$) time-lapse imaging series (out of n = 9) with 1 Hz imaging intervals is displayed. Five repetitive −200 mV (hyperpolarization) voltage pulses followed by five +60 mV (depolarization) voltage pulses were applied with an interval of 15 sec, followed by a continuous series of −200 mV pulses with an interval of 20 sec as indicated by the upper bars. Application of 100 μM $LaCl_3$ as pointed out by the bar abolished the repetitive decrease in anion-ratio signal at the tip. The presence of Lanthanum did not influence the −200 mV-induced rhythmic decrease of the ratio signal at the electrode insertion site indicating a Ca^{2+}-leak there. Note that the presence of $LaCl_3$ increased the overall anion concentration, a cause of blocking Ca^{2+}-permeable channels and thus Ca^{2+}-signaling for anion release.
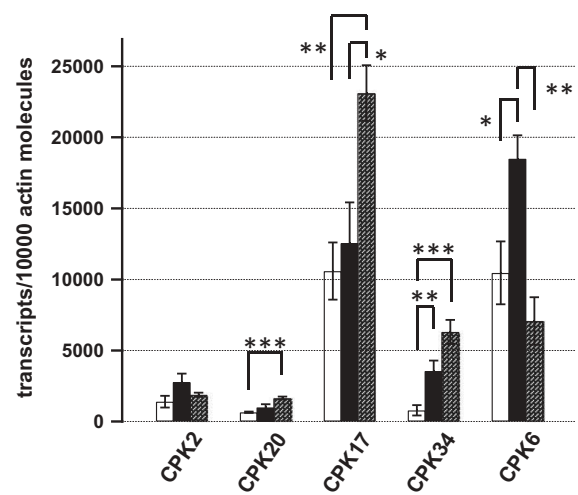
(A)
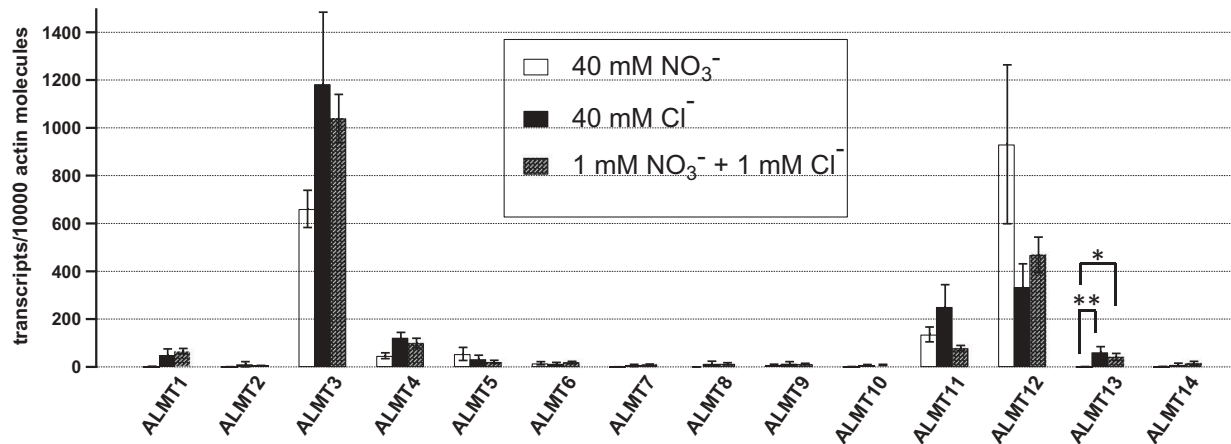
(B)
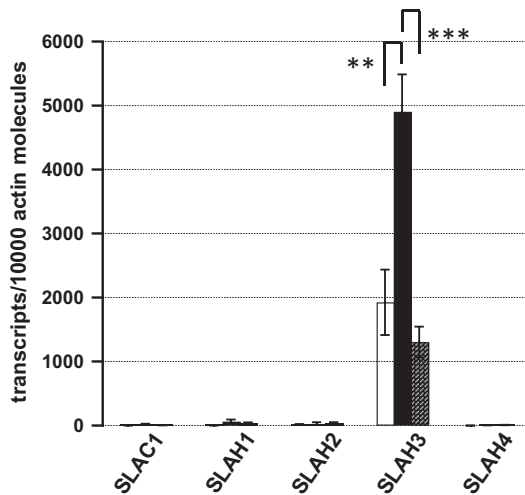
(C)

Figure 2. Interrelation between anion channel and CPK expression levels in different pollen tube growth conditions. A quantification of PT transcripts of all (A) R- and (B) S-type anion channels as well as (C) selected CPKs was performed by qRT-PCR on PT cDNA grown in three distinct media containing different anion concentrations (each n = 6). The semi-solid growth medium consisted of (in mM): 1.6 H_3BO_3, 1 MES/pH 5.8 with TRIS and either 20 $Ca(NO_3^-)_2$ (white bar), 20 $CaCl_2$ (black bar) or 0.5 $Ca(NO_3^-)_2$ + 0.5 $CaCl_2$ + 19 Ca^{2+}-Gluconate (patterned bar). Asterisks *, ** and *** indicate unpaired t test values of $p < 0.05$, $p < 0.005$ and $p < 0.0005$, respectively.

high NO_3^- and Cl^-/NO_3^- minimal medium (Figure 2B, $p < 0.0033$ and $p < 0.0002$). The same transcript profile was apparent with *CPK6*, which is known to activate ALMT12/14 and SLAH3.[8,18] A significant upregulation of *CPK6* transcript numbers in high Cl^- medium in contrast to the high NO_3^- and minimal medium was detected (Figure 2C, $p < 0.0152$ and $p < 0.0006$). Transcript levels of the SLAH3 and ALMT12 activating kinase CPK20 were 16–18 fold smaller than the ones of CPK6. Compared to *CPK6*, the expression profile of *CPK20* was very different and characterized by lowest transcript levels in high NO_3^-. *CPK20* transcript levels were upregulated in high Cl^- and Cl^-/NO_3^- minimal medium ($p < 0.001$). The transcript profile of *CPK17* and *CPK34*, two kinases important for fertilization[19] with yet unidentified physiological substrates, was similar to the *CPK20* profile but their transcript numbers were 4–12 times higher (Figure 2C).

Discussion

Within this work we could substantiate and validate the importance of the Ca^{2+}-dependent activation of R- and S-type anion channels for the regulation of PT growth. The application of 1 sec lasting −200 mV voltage pulses was shown to induce a reproducible reduction in [anion]$_{cyt}$ at the tip, which were held off in the presence of the Ca^{2+}-permeable channel inhibitor Lanthanum. The voltage-dependency of anion channels is unlikely to account for the tip [anion]$_{cyt}$ decrease during the −200 mV pulses, because the same pulses were applied in the presence of Lanthanum. The most reasonable explanation is a missing Ca^{2+}-signaling for anion channel activation and in turn anion efflux at the PT tip by the use of Lanthanum. Additionally, Lanthanum increased the [anion]$_{cyt}$ 20–80 µm behind the tip, indicative for an anion uptake mechanisms at the shank via a yet unknown transport system

(Figure 1). Within the framework of this manuscript, a correlation of CPK and anion channel expression profiles was demonstrated via qRT-PCR (Figure 2). CPK2 and CPK6, known SLAH3 activators show very similar or even the same expression profile as the S-type anion channel in all growth media tested. It is tempting to speculate that the bulk anion efflux via anion channels could be regulated transcriptionally according to their permeability properties and regulation via CPKs. The relative permeability ratio of SLAH3 for NO_3^-:Cl^- was determined recently in *Xenopus laevis* oocytes to be 20:1.[15] In contrast, ALMT12 is highly permeable to malate and to a less extent to Cl^-, SO_4^{2-} [16] and NO_3^-.[17] Relative high expression of SLAH3 as well as CPK2 and CPK6 in 40 mM Cl^- medium might suggest a mechanism to compensate for the minor Cl^- conductivity of SLAH3 (Figure 2). Furthermore, the high NO_3^- permeability and activation mechanism of SLAH3 by extracellular NO_3^- [15] might be reflected in the smaller SLAH3 transcript numbers in the high NO_3^- medium compared to the high Cl^- medium. In addition, the low Cl^- permeability of SLAH3 might be compensated by higher CPK6 transcript abundancy, known to activate ALMT12 and SLAH3[8] in order to maintain bulk anion flow. The significant permeability of ALMT12 for Cl^- and NO_3^- [8,17] might suggest an active regulation of R-type anion channel(s) activity when SLAH3 transcript abundancy decreases, or when the highly permeable organic anion malate, known to increase ALMT clade III expression,[8] is present.

Besides the essential role for anion efflux at the tip, we still do not exactly know its physiological role for polar growth. It is speculated that Ca^{2+}-dependent anion channel activity induces a local membrane depolarization[20] and that the apical anion gradient is important for vesicle transport to the tip.[21] Generally it is assumed that the high tip $[Ca^{2+}]_{cyt}$ governs vesicle fusion for cell growth at the extreme apex like in animal or fungal systems.[22–24] However, the route for vesicle transport to the plasma membrane at the PT tip for exocytosis is still controversially discussed.[25] The absence of a functional cytoskeleton network in the extreme apex of PTs[26] for coordinated vesicle trafficking tip-wards represents the motivation for the osmophoresis model.[21] This model argues for a directed vesicle movement based on the cytosolic anion and in turn osmotic gradient within the tip region that may explain the delivery of exocytosis vesicles to the plasma membrane at the tip.[21] While this hypothesis has not yet been experimentally validated, it might account for the tight coupling of the tip $[Ca^{2+}]_{cyt}$ and $[anion]_{cyt}$ described recently,[8,9] and corroborated in this manuscript. It is worthwhile to hypothesize that Ca^{2+}- and CPK-dependent anion channel activation regulate PT growth by means of this osmophoresis mechanism in concert with a process called self-electrophoresis. The self-electrophoresis model is based on a voltage gradient along the cell that is thought to attract charged molecules in a cellular electric field.[27] The local Ca^{2+}-driven anion channel activation likely facilitates enough charge movement[10] to generate a gradient in membrane voltage to account for the electric field that was already described.[28] and known to play a role in PT orientation.[29,30] In agreement with this idea, membrane voltage oscillations and depolarization of intact guard cells and protoplasts thereof have been reported to depend on anion channel activity.[31,32] Latest progress in the field of electrotropism and polarity establishment of cells and tissues via electric cues is in line with the self-electrophoresis model.[33,34] Future work on this very interesting topic will shed light on electric signaling within PTs to steer polar growth and guidance.

Materials and methods

Growth conditions of *N. tabacum* and *A. thaliana* plants used here have been explained elsewhere.[9] Simultaneous voltage-clamp and anion imaging of *N. tabacum* PTs expressing the Cl^--sensor[14] was performed as described in Gutermuth et al., 2013; 2018. The qRT-PCR primers used, quantification of transcript numbers (qRT-PCR) and statistical analysis were carried out as depicted in Gutermuth et al., 2013; 2018. The reference genes to normalize transcript numbers were actin 2/8. Pollen of wild-type Col-0 plants were harvested with the vacuum cleaner technique. 4–6 hours after pollen containing gaze was placed on designated semi-solid growth medium, RNA was isolated according to Gutermuth et al., 2013, 2018. Additional primers used here for transcript quantification of CPKs are: CPK2 fwd GTACAGATTGACGGTG, CPK rev GTCCGGGGTGAT AAAG, CPK6 fwd TGCTGGTGTAGGGAGAA, CPK6 rev CCTCACAGCTACTGATGAA, CPK17 fwd TTACATCGC ACCTGAG, CPK17 rev CCACTACTATCAGTATCC, CPK20 fwd AGTCCTTATTATGTGGC, CPK20 rev GTGATGTG TCCACTAT, CPK34 fwd GCTAGGTCGTGGACAG, CPK34 rev ATCGTCCGTAGTAACGAG. qRT-PCR was performed on cDNA from *Arabidopsis* wild-type Col-0 PTs grown for 4–5 hours either on a minimal medium with 1 mM NO_3^-/Cl^- each or containing high (40 mM) NO_3^- or Cl^- concentrations. Minimal medium consisted of 0.5 mM $CaNO_3$, 0.5 mM $CaCl_2$ and 19 mM Ca-Gluconate. The high NO_3^- or Cl^- medium contained 20 mM $Ca(NO_3)_2$ and 20 mM $CaCl_2$, respectively.

Author contributions

TG, SH and KRK performed the experiments, analyzed data and prepared the figures. The project was proposed and supervised by KRK, who wrote and prepared the manuscript.

Accession Numbers

Sequence data from this article can be found in the Arabidopsis Genome Initiative or GenBank/EMBL databases under the following accession numbers: SLAC1:At1g12480 (Q9LD83), SLAH1:At1g62280 (Q9FLV9), SLAH2: At4g27970 (Q9ASQ7), SLAH3:AT5G24030 (Q9FLV9), SLAH4:At1g62262

(A8MRV9), ALMT1:At4g00910 (Q9SJE9.1), ALMT2:At1g08440 (Q9SJE8.2), ALMT3:At1g18420 (Q9LPQ8.1), ALMT4:At1g25480 (Q9C6L8.1), ALMT5: At1g68600 (Q93Z29.1), ALMT6:At2g17470 (Q9SHM1.1), ALMT7: At2g 27240 (Q9XIN1.1), ALMT8:At3g11680 (Q9SRM9.1), ALMT9:At3g18440 (Q9LS46.1), ALMT10:At4g00910 (AEE81955.2), ALMT11:At4g17585 (Q3E9 Z9.1), ALMT12:At4g17970 (O49696), ALMT13:At5g46600 (Q9LS23.1), ALMT14:At5g46610 (Q9LS22.1), CPK2:At3g10660 (Q38870), CPK6: At2g17290 (Q38872), CPK17:At5g12180 (Q9FMP5), CPK20:At2g38910 (Q9ZV15) and CPK34:At5g19360 (Q3E9C0).

ORCID

Kai Robert Konrad 🔗 http://orcid.org/0000-0003-4626-5429

References

1. Konrad KR, Maierhofer T, Hedrich R. Spatio-temporal aspects of Ca^{2+} signalling: lessons from guard cells and pollen tubes. J Exp Bot. 2018;69:4195–4214.
2. Konrad KR, Wudick MM, Feijó JA. Calcium regulation of tip growth: new genes for old mechanisms. Curr Opin Plant Biol. 2011;14:721–730. doi:10.1016/j.pbi.2011.09.005.
3. Gao QF, Gu LL, Wang HQ, Fei CF, Fang X, Hussain J, Sun S-J, Dong J-Y, Liu H, Wang Y-F Cyclic nucleotide-gated channel 18 is an essential Ca^{2+} channel in pollen tube tips for pollen tube guidance to ovules in *Arabidopsis*. Proceedings of the National Academy of Sciences of the United States of America 2016; 113:3096–3101. doi:10.1073/pnas.1524629113.
4. Michard E, Lima PT, Borges F, Silva AC, Portes MT, Carvalho JE, Gilliham M, Liu L-H, Obermeyer G, Feijó JA. Glutamate receptor-like genes form Ca^{2+} channels in pollen tubes and are regulated by pistil D-serine. Science. 2011;332:434–437. doi:10.1126/science.1201101.
5. Qu HY, Shang ZL, Zhang SL, Liu LM, Wu JY. Identification of hyperpolarization-activated calcium channels in apical pollen tubes of *Pyrus pyrifolia*. New Phytologist. 2007;174:524–536. doi:10.1111/j.1469-8137.2007.02069.x.
6. Shang ZL, Ma LG, Zhang HL, He RR, Wang XC, Cui SJ, Sun D-Y. Ca^{2+} influx into lily pollen grains through a hyperpolarization-activated Ca^{2+}-permeable channel which can be regulated by extracellular CaM. Plant Physiol. 2005;46:598–608. doi:10.1093/pcp/pci063.
7. Wu J, Shang Z, Jiang X, Moschou PN, Sun W, Roubelakis-Angelakis KA, Roubelakis-Angelakis KA, Zhang S. Spermidine oxidase-derived H_2O_2 regulates pollen plasma membrane hyperpolarization-activated Ca^{2+}-permeable channels and pollen tube growth. Plant J. 2010;63:1042–1053. doi:10.1111/j.1365-313X.2010.04301.x.
8. Gutermuth T, Herbell S, Lassig R, Brosche M, Romeis T, Feijo JA, Hedrich R, Konrad KR. Tip-localized Ca^{2+}-permeable channels control pollen tube growth via kinase-dependent R- and S-type anion channel regulation. New Phytol. 2018;218:1089–1105. doi:10.1111/nph.15067.
9. Gutermuth T, Lassig R, Portes M-T, Maierhofer T, Romeis T, Borst J-W, Hedrich R, Feijo JA, Konrad KR. Pollen tube growth regulation by free anions depends on the interaction between the anion channel SLAH3 and calcium-dependent protein kinases CPK2 and CPK20. Plant Cell Online. 2013;25:4525–4543. doi:10.1105/tpc.113.118463.
10. Zonia L, Cordeiro S, Tupy J, Feijó JA. Oscillatory chloride efflux at the pollen tube apex has a role in growth and cell volume regulation and is targeted by inositol 3,4,5,6-tetrakisphosphate. Plant Cell. 2002;14:2233–2249.
11. Breygina MA, Matveyeva NP, Andreyuk DS, Yermakov IP. Transmembrane transport of K^+ and Cl^- during pollen grain activation *in vivo* and *in vitro*. Russian J Dev Biol. 2012;43:85–93. doi:10.1134/S1062360412020038.
12. Tsien RW, Hess P, McCleskey EW, Rosenberg RL. Mechanisms of selectivity, permeation, and block. Annu Rev Biophys Biophys

Chem. 1987;16:265–290. doi:10.1146/annurev.bb.16.060187.001405.
13. Tester M. Tansley review no. 21 plant ion channels: whole-cell and single channel studies. New Phytologist. 1990;114:305–340. doi:10.1111/nph.1990.114.issue-3.
14. Markova O, Mukhtarov M, Real E, Jacob Y, Bregestovski P. Genetically encoded chloride indicator with improved sensitivity. J Neurosci Methods. 2008;170:67–76. doi:10.1016/j.jneumeth.2007.12.016.
15. Geiger D, Maierhofer T, AL-Rasheid KAS, Scherzer S, Mumm P, Liese A, Ache P, Wellmann C, Marten I, Grill E, et al. Stomatal closure by fast abscisic acid signaling is mediated by the guard cell anion channel SLAH3 and the receptor RCAR1. Sci Signal. 2011;4: ra32-. doi:10.1126/scisignal.2001346.
16. Meyer S, Mumm P, Imes D, Endler A, Weder B, Al-Rasheid KA, Geiger D, Marten I, Martinoia E, Hedrich R. AtALMT12 represents an R-type anion channel required for stomatal movement in Arabidopsis guard cells. Plant J. 2010;63:1054–1062. doi:10.1111/j.1365-313X.2010.04302.x.
17. Sasaki T, Mori IC, Furuichi T, Munemasa S, Toyooka K, Matsuoka K, Murata Y, Yamamoto Y. Closing plant stomata requires a homolog of an aluminum-activated malate transporter. Plant Cell Physiol. 2010;51:354–365. doi:10.1093/pcp/pcq016.
18. Scherzer S, Maierhofer T, Al-Rasheid KA, Geiger D, Hedrich R. Multiple calcium-dependent kinases modulate ABA-activated guard cell anion channels. Mol Plant. 2012;5:1409–1412. doi:10.1093/mp/sss084.
19. Myers C, Romanowsky SM, Barron YD, Garg S, Azuse CL, Curran A, Davis RM, Hatton J, Harmon AC, Harper JF. Calcium-dependent protein kinases regulate polarized tip growth in pollen tubes. Plant J. 2009;59:528–539. doi:10.1111/j.1365-313X.2009.03894.x.
20. Michard E, Simon AA, Tavares B, Wudick MM, Feijó JA. Signaling with ions: the keystone for apical cell growth and morphogenesis in pollen tubes. Plant Physiol. 2017;173:91–111. doi:10.1104/pp.16.01561.
21. Lipchinsky A. Osmophoresis - a possible mechanism for vesicle trafficking in tip-growing cells. Phys Biol. 2015;12:066012. doi:10.1088/1478-3975/12/6/066012.
22. Neher E, Sakaba T. Multiple roles of calcium ions in the regulation of neurotransmitter release. Neuron. 2008;59:861–872. doi:10.1016/j.neuron.2008.08.019.
23. Sutter J-U, Denecke J, Thiel G. Synthesis of vesicle cargo determines amplitude of Ca^{2+}-sensitive exocytosis. Cell Calcium. 2012;52:283–288. doi:10.1016/j.ceca.2012.05.011.
24. Takeshita N, Evangelinos M, Zhou L, Serizawa T, Somera-Fajardo RA, Lu L, Takaya N, Nienhaus GU, Fischer R Pulses of Ca^{2+} coordinate actin assembly and exocytosis for stepwise cell extension. Proceedings of the National Academy of Sciences 2017; 114:5701–5706. doi:10.1073/pnas.1700204114.
25. Grebnev G, Ntefidou M, Kost B. Secretion and endocytosis in pollen tubes: models of tip growth in the spot light. Front Plant Sci. 2017;8. doi:10.3389/fpls.2017.00154.
26. Qu X, Jiang Y, Chang M, Liu X, Zhang R, Huang S. Organization and regulation of the actin cytoskeleton in the pollen tube. Front Plant Sci. 2015;5:786.
27. Jaffe LF, Robinson KR, Nuccitelli R. Local cation entry and self-electrophoresis as an intracellular localization mechanism. Ann N Y Acad Sci. 1974;238:372–389.
28. Weisenseel MH, Nuccitelli R, Jaffe LF. Large electrical currents traverse growing pollen tubes. J Biol. 1975;66:556–567.
29. Nozue K, Wada M. Electrotropism of Nicotiana pollen tubes. Plant Physiol. 1993;34:1291–1296.
30. Malho R, Feijo JA, Pais MSS. Effect of electrical fields and external ionic currents on pollen-tube orientation. Sex Plant Reprod. 1992;5:57–63. doi:10.1007/BF00714558.
31. Konrad KR, Hedrich R. The use of voltage-sensitive dyes to monitor signal-induced changes in membrane potential - ABA

triggered membrane depolarization in guard cells. Plant J. 2008;55:161–173. doi:10.1111/j.1365-313X.2008.03498.x.

32. Raschke K, Shabahang M, Wolf R. The slow and the quick anion conductance in whole guard cells: their voltage-dependent alternation, and the modulation of their activities by abscisic acid and CO_2. Planta. 2003;217:639–650. doi:10.1007/s00425-003-1033-4.

33. Allen Greg M, Mogilner A, Theriot Julie A. Electrophoresis of cellular membrane components creates the directional cue guiding keratocyte galvanotaxis. Curr Biol. 2013;23:560–568. doi:10.1016/j.cub.2013.02.047.

34. Chang F, Minc N. Electrochemical control of cell and tissue polarity. Annu Rev Cell Dev Biol. 2014;30:317–336. doi:10.1146/annurev-cellbio-100913-013357.